International Journal of Current Engineering and Technology

ISSN 2277 – 4106

Available at http://inpressco.com/category/ijcet

Research Article

High Permittivity Poly (methyl methacrylate)/Sr_2TiMnO_6 Composites for high energy storage capacitor application.

P.Thomas[a] ,B.S.Dakshayini [b] and G.K.Mahadevaraju.[b]

[a]Dielectric Materials Division, Central Power Research Institute, Bangalore : 560 080, India
[b]Department of Chemical Engineering, Dayananda Sagar College of Engineering, Bangalore: 560012,India

Abstract

High permittivity Poly (Methyl Methacrylate) (PMMA) and Sr_2TiMnO_6 (STMO) composites were fabricated via melt mixing followed by hot pressing technique. These were characterized using X-ray diffraction (XRD), Scanning electron microscopy (SEM), thermo gravimetric (TGA), Density, Hardness, electrical properties like Volume resistivity, Permittivity and AC conductivity. SEM revealed that the crystallites are well distributed and the porosity is almost negligible. Both density and hardness were improved as the STMO content increased in the PMMA matrix. Addition of STMO in PMMA reduces the resistivity of the composite due to the increase in the conductivity of the composite as revealed by the AC conductivity. Permittivity values as high as 23 @ 100 Hz has been achieved (PMMA+STMO-50%), demonstrating that this PMMA+STMO composite can be exploited for the fabrication of high energy storage capacitor application.

Keywords: *Poly(Methyl Methacrylate) (PMMA): $CaCu_3Ti_4O_{12}$ (CCTO): Polymer composite: Melt: SEM: Thermogravimetric: Dielectric Properties.*

Introduction

Ceramic-polymer composites have attracted considerable attention due to the potential combination of the advanced properties of inorganic and organic components (R. Shenhar etal, 2005). The integration of embedded passive components into printed circuit boards offers a significant reduction in size, an improved electrical performance and reliability, faster switching speed, and lower costs (Y. Rao et al, 2002, S. Ogitani et al, 2000, R.E. Newnham et al, 1978, S.K. Bhattacharya et al, 2000). Among the embedded passive components such as resistor, capacitor, and inductor, an embedded capacitor plays an important role as a coupling or bypasses capacitor on circuits and occupies more than 40% of the passive components (Y. Rao et al, 2002, S.K. Bhattacharya et al, 2000). Nowadays, there is much interest in finding materials with tailored electrical properties to efficiently work as dielectrics, insulators for high voltage applications and piezoelectric for sensors and actuators (A. Facchetti et al, 2005, Y. Bai et al, 2000, Q.M. Zhang, 2002). Depending on their final application, these materials may require high dielectric constant and/or high dielectric strength, at the same time being easy to process and dimensionally stable in order to manufacture devices with complex geometries and small sizes for real applications in integrated circuits (J.X. Lu et al, 2008). Because of their high dielectric constants, ferroelectric ceramics (barium titanate ($BaTiO_3$), barium strontium titanate ($BaSrTiO_3$), lead titanate zirconate ($PbZrTiO_3$), etc.) with permanent dipole moments are, in principle, good candidates for this sort of application. However, with this kind of material high processing temperatures might be required which is unsuitable, for example, in printed circuit manufacturing. On the other hand, polymer dielectrics are more compatible when using relatively low processing temperatures but, unfortunately, they have too low dielectric constants to attain very high capacitances. With the aim of increasing the ε'_r values in polymer materials, preparation of composites is a good choice. Therefore, it seems reasonable to combine the advantages of polymers, such as low processing temperatures, mechanical flexibility and low price, with those of different kinds of filler (inorganic particles), for instance specific electrical properties.The most widely used high permittivity ceramic-polymer composites are those based on ferroelectric $BaTiO_3$(BT), $BaSrTiO_3$(BST),$Pb(Mg_{1/3}Nb_{2/3})O_3$-$PbTiO_3$(PMNPT), and $Pb(Zr,Ti)O_3$(PZT) (R.Gregorio et al, 1996, S.U. Adikary et al, 2002, Z.M. Dang et al, 2003, P. Kim et al, 2007). Recently, the $CaCu_3Ti_4O_{12}$ (CCTO) ceramic has gained considerable attention due to its large permittivity ($\varepsilon \sim 10^{4-5}$) (M.A. Subramanian et al, 2000) and has been used as a filler and studied (M. Arbatti et al, 2007, P. Thomas et al, 2010, P. Thomas et al, 2012) to explore the possibility of obtaining a new generation composites associated with high permittivity for capacitor applications in electrical circuits.

*Corresponding author: **P.Thomas**

Double perovsites have attracted considerable attention due to their unique electrical and magnetic properties. Sr_2TiMnO_6 (STMO) ceramic belongs to a family that can be represented by formula $A_2B'B''O$ where the A site is occupied by alkaline earth metals such as Ca, Ba, Sr etc. or rare earth ions of larger ionic radii, B′ and B″ octahedral sites are occupied by the transition metal cations with smaller ionic radii (K.R.S. Preethi Meher et al, 2010). The dielectric constant was found to vary significantly with the thickness of the samples and nature of the contacts at low frequencies owing to its extrinsic nature (K.R.S. Preethi Meher et al, 2009). The Poly (methyl methacrylate) (PMMA), a transparent thermoplastic polymer, possesses moderate physical properties associated with low cost and composite systems based on this were studied in great detail (A. Edurd et al, 2010, Hong Wang et al, 2010, Ziad Khattari et al, 2012). These results suggest that one could chose PMMA combined with giant permittivity ceramics such as STMO for the fabrication of composites with high permittivity for the energy storage applications. In this paper, we report the details pertaining to the fabrication and characterization of PMMA/STMO composite by melt mixing and hot pressing technique.

Experimental

The solid-state reaction route was adopted for synthesizing STMO ceramic powders. The stoichiometric amounts of AR grade $SrCO_3$, MnO_2 and TiO_2 was weighed, mixed using acetone and ball milled (300 rpm) for 3h. The homogeneous mixture thus obtained was dried in an electric oven for about 1h. This stoichiometric mixture was taken in a re-crystallizedalumina crucible and heated at 1200^{o}C for 24 h, followed by furnace cooling. The samples were again calcined at 1370^{o}C for about 24 h to obtain phase pure STMO powder. In order to get submicron particles, the STMO powders were ball milled for about 4h using a planetary mill. PMMA, having Molecular weight of 1,10,000, (Make: LG Corporation) was used as matrix material. For the fabrication of composites, initially, the as received PMMA granules were heated at 210^{o}C in Brabender Plasticorder (Model:PLE331) till the PMMA granules are thoroughly melted. To this melt, STMO powder (0 to 50 % by weight) was slowly added and mixed for 20 min at this temperature. The mixture was taken out from the Plasticorder and hot-pressed at this temperature to obtain a sheet of 100 mm^2 with 1.0 mm in thickness. A series of STMO/PMMA composites were fabricated. The composite become brittle when the ceramic loading was beyond 50 % by weight. Hence, to obtain flexible composite which could be made into a variety of shapes, the ceramic loading has been restricted to maximum of 50 wt %. To examine the structure, an XPERT-PRO Diffractometer (Philips, Netherlands) was used. The scanning electron microscopy (SEM) measurement was carried out using Leica SEM instrument. Thermo gravimetric (TGA) analyses were done using the TA Instruments (UK, Model: TGA Q500). TGA experiments were conducted in Nitrogen atmosphere at a flow rate of 60ml/min, at a heating rate of 10 deg/min. The densities of the composites were measured by Archimedes liquid displacement method. The hardness test was carried out as per the procedure outlined in the ASTM D 2240 . The volume resistivity was characterized as per the procedure outline in ASTM D257. An LCR meter (Model: HP4194A) was used for the capacitance measurements as a function of frequency (100Hz–110MHz) at room temperature.The measurement accuracy of the instrument is less than 5%. The dielectric constant was calculated using the relation$\varepsilon_r = c \times d \,/\, \varepsilon_0 A$, where *c*iscapacitance, *d*is the thickness of the sample,ε_0= 8.854X10^{-12} F/m and A is the electrode area of the sample. These results are given in the Table.1.

Results and Discussion

X-Ray diffraction studies

Fig.1 shows the XRD pattern recorded for the Sr_2TiMnO_6 (STMO) prepared by solid state chemistry route. It has been observed that Fig.1(a), there are secondary phases pertaining to $SrMnO_3$, $SrTiO_3$ and TiO_2 for the sample calcined at 1200^{o}C Hence, the calcination temperature was enhanced to 1300^{o}C to obtain phase pure STMO, the XRD pattern obtained for this sample is shown in Fig.1(b). As there are secondary phases of $SrMnO_3$, $SrTiO_3$ and TiO_2, this result implies that the phase pure STMO would be obtained only above 1350^{o}C. It has been observed that, phase pure STMO is obtained when the ceramic was calcined at 1370^{o}C Fig.1(c), which is consistent with the results reported (K.R.S. Preethi Meher et al, 2010).The X-ray diffraction patterns were recorded on the STMO ceramic powders, as received PMMA and on the composites that were fabricated. X-ray diffraction pattern revealed that the as received PMMA is semi crystalline in nature Fig.2(a). The X-ray diffraction pattern recorded for the PMMA comprising 10 wt% STMO Fig.2(b), revealed its composite nature. In the case of PMMA with 50 wt% STMO composite Fig.2(f), XRD pattern revealed only STMO peaks as the intensities of these are dominant.

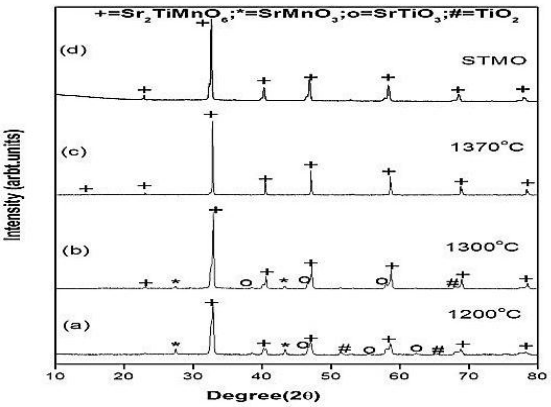

Figure.1: XRD pattern recorded for STMO calcined at (a) 1200^{o}C, (b) 1300^{o}C, (c) 1370^{o}C and (d) STMO reported in literature (K.R.S. Preethi Meher , 2010).

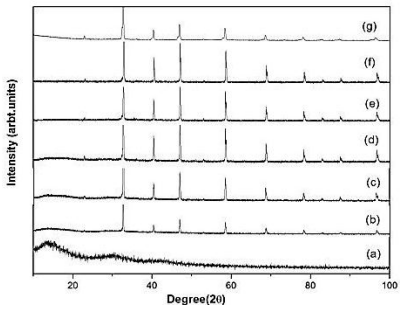

Figure.2: XRD pattern for (a) Pure PMMA, (b) PMMA+STMO-10%, (c) PMMA+STMO-20%, (d)PMMA+STMO-30%, (e) PMMA+STMO-40%, (f)PMMA+STMO-50%, and (g) STMO(K.R.S. Preethi Meher , 2010).

Thermal studies (TGA)

The Thermo gravimetric analysis was carried as per the procedure outline in the ASTM standard (ASTM D, 3850-94) . In order to examine the thermal stability, thermal analyses were carried out on PMMA+STMO composites as well as on pure PMMA for comparison. Fig.3(a-f) shows the thermograph recorded for the pure PMMA and for PMMA+STMO composites (10 to 50 wt%). It has been observed that there is a change in the thermal degradation behaviour of PMMA with STMO. The onset of decomposition temperature has increased as the STMO filler content increased in PMMA. The onset of decomposition temperature (temperature at 10% weight loss) (C. Marius et al, 2006) was found to increase for all the composites under study. The decomposition temperature onset accompanied by 10% weight loss for PMMA+STMO-10wt% is 354.75^{o}C and for the PMMA+STMO-50 wt%, is 363.69^{o}C, while for pure PMMA, it is 353.5^{o}C. The onset of decomposition temperature is higher by 10^{o}C than that of virgin PMMA. All the samples (PMMA and composites) indicated that there is no weight loss upto 270^{o}C and thereafter, the degradation begins.

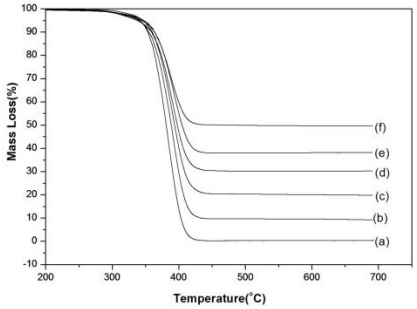

Figure.3:TGAthermogramfor(a)purePMMA,(b)PMMA+STMO-10%, (c)PMMA+STMO-20%, (d) PMMA+STMO-30%, (e) PMMA+STMO-40%, and (f) PMMA+STMO-50% composites.

Microstructural studies

The scanning electron microscopy (SEM) measurement was carried out using Leica SEM instrument in order to analyse the dispersion of ceramic STMO in the PMMA matrix. Fig.4(a & b) illustrates the SEM micrographs recorded on the fractured samples containing 10, 20, 30, 40 & 50 wt % of STMO in PMMA. It is seen that in Fig.4(a) the crystallites are randomly distributed in the PMMA+STMO-10wt% composite. In the case of PMMA+STMO-50wt % composite Fig.4(b), the crystallites are well distributed and the porosity is almost negligible implying that the fabrication of composites with good dispersion of ceramic particles into the polymer matrix has been achieved.

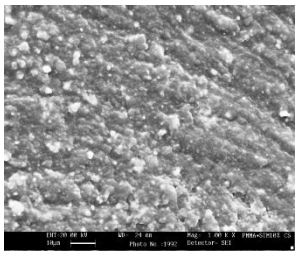

Figure.4(a): Scanning Electron Micrographs of PMMA+ STMO-10% composite.

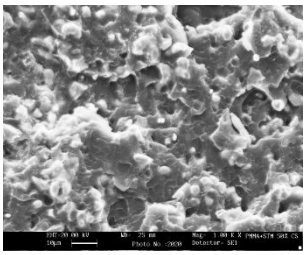

Figure.4(b): Scanning Elect--tron Micrographs PMMA+ STMO - 50% composite.

Density

The density measurements were carried out as per the procedure outlined in the ASTM standard (ASTM D 792). The weight of the sample in air and weight of the sample in water is noted and density is calculated using the following equation,

$$\rho_{sample} = \frac{Wa}{W_a - W_1} \times \rho_{water} \quad (1)$$

Where ρ is the density of the sample, W_a the weight of the sample in air, W_1 the weight of the sample in water. The effect of STMO ceramic on the density of the PMMA material has been studied. Density of the pure PMMA increased when the STMO content increased in PMMA. The pure PMMA has the density (g/cc) of about 1.180, which has increased to 1.9415 when the STMO content is increased to 50 wt% in PMMA. The Fig.5 shows the variation of density as a function of the STMO filler loading. When the density is plotted against composition (Fig.5), it is clearly seen that the density of the composite increases gradually with the increase in STMO filler loading.

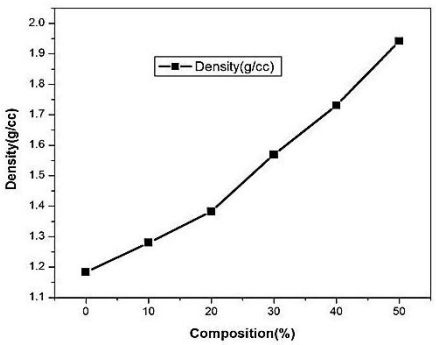

.

Figure.5: Variation of density as a function of wt% of STMO for PMMA+STMO composite PMMA/STMO composite.

Hardness

The hardness test was carried out as per the procedure outlined in the ASTM standard (ASTM D 2240). Fig.6 gives the variation of Hardness as a function of wt% of STMO for PMMA+STMO composite. The hardness of the material increases as the STMO content increased in the PMMA matrix. There is a linear increase in Hardness from 61 to 79 (Shore D) value as the STMO content increases from 0 to 50 wt% in the PMMA matrix. These results indicate that the hardness in an composite has a linear relationship with the density (g/cc) of the composite. In an essence, material with improved density, will exhibit increased hardness.

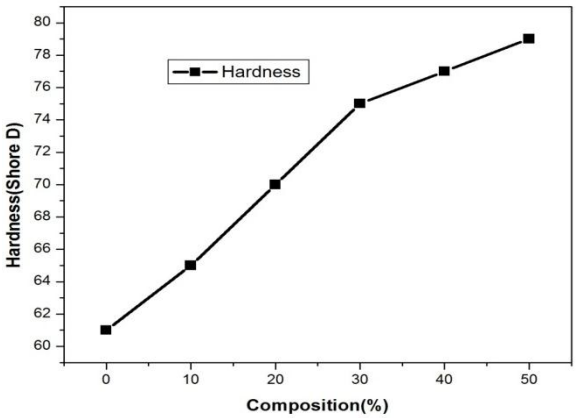

Figure. 6: Variation of hardness as a function of wt% of STMO for PMMA+STM composite PMMA/STMO composite.

Frequency dependence of room temperature Permittivity

The Fig.7 shows the permittivity and loss recorded for the pure PMMA obtained from the melt mix and hot pressing. It is seen that the permittivity is around 4.9@100 Hz and constant over the frequency under investigation (100 Hz to 100 MHz). The dielectric loss also exhibited the similar behavior. The room temperature permittivity data obtained for PMMA+STMO composites for different wt% of STMO are given in Fig.8. As expected, when the STMO content increased in PMMA. The permittivity had increased. When the STMO content increased to 50 wt% in PMMA, the permittivity value of PMMA had increased to 22.6 @ 100 Hz from 4.9 @ 100 Hz. Similar trends have been obtained in the case of PMMA+CCTO composite also. The permittivity values increased to 15.7 @100 Hz for 38 vol% of CCTO in PMMA (P. Thomas et al, 2012). Introduction of Al_2O_3 in PMMA to the level of 45 vol% has increased the permittivity, which has been attributed to the space charge polarization mechanism (Bahaa Hussien, 2011).

The room temperature dielectric loss data obtained for PMMA+STMO composites for different wt% of STMO are given in Fig.9. The dielectric loss for all the composite lies below 0.018 for the entire frequency range under investigations. At low frequency, space charge polarization is dominant (Bahaa Hussien, 2011).

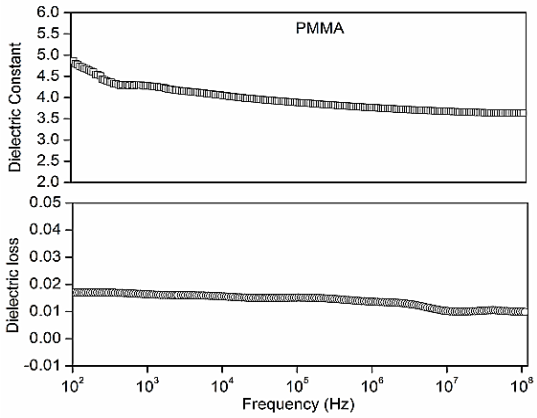

Figure.7: Frequency dependent dielectric constant and dielectric loss measured at room temperature (300K) for pure PMMA.

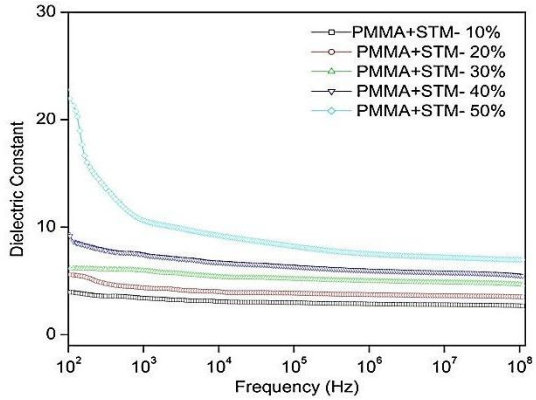

Figure.8: Frequency dependence of dielectric constant measured at room temperature (300K) for different weight percent of STMO in PMMA.

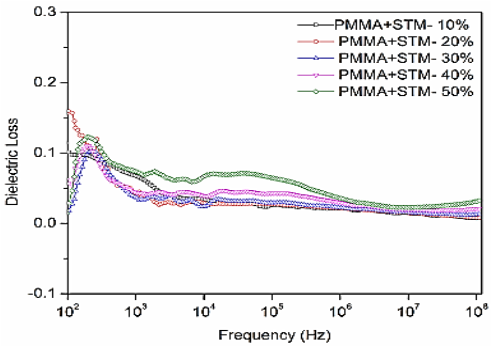

Figure.9: Frequency dependence of dielectric loss measured at room temperature (300K) for different weight percent of STMO in PMMA.

Volume resistivity

Volume resistivity is the ratio of the potential gradient parallel to the current along its surface to the current per unit width of the surface. The pure PMMA and the composites were characterized for the volume resistivity as per the procedure outline in ASTMstandard (ASTM D257). The PMMA and composites were subjected to volume resistivity measurement under different applied

voltages, 500V, 1000V and 1500V. The volume resistivity was calculated using the equation,

VR= R_v A/d (2)

Where VR = Volume resistivity (ohm-cm), R_v= Resistance of the material to the flow of charge (ohm), d = Sample thickness (cm),A = measuring electrode area (cm^2) = 7.1$cm^{2.}$

Fig.10 shows the variation of volume resistivity with composition as a function of applied voltage. The volume resistivity of the PMMA had slightly increased on the addition of 10% wt. % of STMO. This is due to the fact that the dielectric constant of the PMMA+STM-10 composite (Fig.10) is only marginal and the improvement in the volume resistivity indicates that the composite is not capacitive in nature. On the other hand, the conductivity of the composite has not been altered much as seen from the AC conductivity. Only when the STMO content increased in the PMMA, the conductivity of the composite increased and hence we observe there is a gradual fall in the resistivity values. Since metals have higher conductivity than the polymers, it has been reported that the addition of metals into the PMMA decreased the resistivity (Vishal Singh et al, 1996, Lei Yang et al, 1994), which supports the fact that the addition of STMO, which is also a high lossy materials, increased the conductivity of the composite and there by reduces the resistivity of the composite.

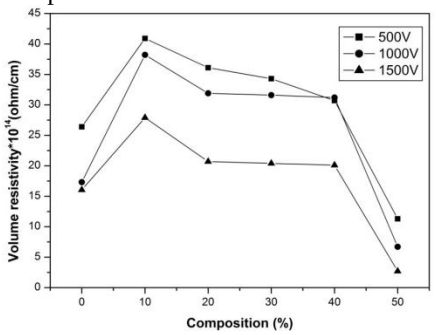

Figure.10: Variation of volume resistivity with composition as a function of applied voltage on PMMA+STMO composites.

A.C. Conductivity

The AC conductivity σ *is* derived from the dielectric data using the equation :

$$\sigma^{'} = \varepsilon_o \omega \varepsilon^{''} \quad (3)$$

where εo = 8.85.10^{-12} F/m is the permittivity of the free space and $\omega = 2\pi f$ the angular frequency. Fig.11 and Fig.12 gives the AC conductivity behavior of pure PMMA and PMMA+STMO composites. It has been observed that the variation of AC conductivity as a function of frequency increases with the frequency for both the PMMA and the composites.

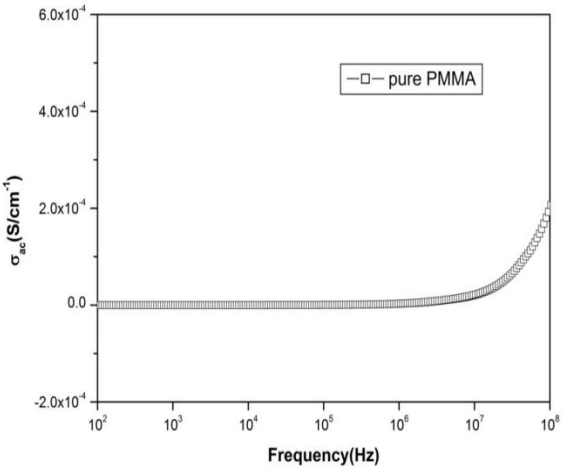

Figure.11: Variation of AC conductivity as a function of frequency measured at room temperature (300K) for pure PMMA.

The composites exhibited higher AC conductivity response than that of the pure PMMA. It has been observed that, the AC conductivity for both PMMA (Fig.11) and composites (Fig.12) increased gradually up to 10 MHz and increased sharply beyond 10 MHz Similar trend have been observed in the case of PMMA +CCTO composite also (P. Thomas et al, 2012).

Table.1. The values of thermal, physical and dielectric properties obtained of pure PMMA and PMMA+STMO composites.

Composition	TGA, Weight loss, (%)	Density gm/cc	Hardness (Shore D)	Vol. Resistivity X 10^{14}ohm/cm			Dielectric Properties @100Hz	
							Permittivity	loss
				500 V	**1000 V**	**1500 V/**	(ε'_r)	
Pure PMMA	99.11	1.183	61	26.4	17.31	16.05	4.9	0.018
PMMA+STMO-10%	89.58	1.28	65	40.9	38.2	27.9	4.04	0.099
PMMA+STMO-20%	79.71	1.383	70	36.1	31.9	20.7	5.48	0.158
PMMA+STMO-30%	69.17	1.5695	75	34.3	31.6	20.4	6.16	0.014
PMMA+STMO-40%	61.36	1.731	77	30.7	31.2	20.1	8.96	0.054
PMMA+STMO-50%	50.43	1.9415	79	11.3	6.7	2.7	22.6	0.029

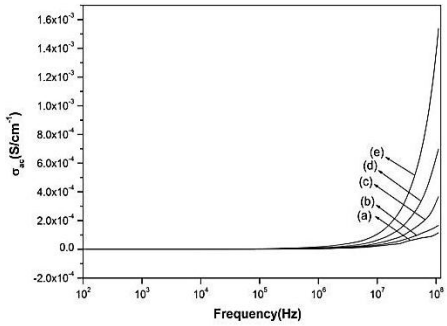

Figure.12: Variation of AC conductivity as a function of frequency measured at room temperature (300K) for (a)PMMA+STMO-10%,(b)PMMA+STMO-20%, (c)PMMA+STMO-30%, (d)PMMA+STMO-40%, and (e)PMMA+STMO-50% composites.

Conclusion

Giant dielectric Sr_2TiMnO_6 (STMO) ceramics were synthesized by solid state route. The single phase nature of the ceramic was confirmed by X-ray diffraction technique. A series of composites (0-50% by wt) were fabricated by incorporating STMO ceramics into the PMMA matrix by melt mixing followed by hot pressing technique. Themicro structural studies by SEM revealed that there is a good dispersion of STMO in the PMMA matrix. Overall, the composite exhibited better thermal stability than that of polymer As expected, permittivity increases as the STMO increased in the PMMA. The permittivity was high as 22.6 @ 100 Hz have been achieved for the PMMA+STM- 50 wt% composite. When the STMO content increased in the PMMA, the conductivity of the composite increased and hence we observe there is a gradual fall in the resistivity values. It has been observed that the variation of AC conductivity as a function of frequency increases with the frequency for both the PMMA and the composites.

Acknowledges

The management of Central Power Research Institute is acknowledged for the financial support (CPRI Project no.R-DMD-01/1415. One of the author (B.S.D), would like to thank CPRI management for giving permission to work for her M.Tech project.

References

A. Eduard, Stefanescu, Xiaoli Tan, Zhiqun Lin, Nicola Bowler, Michael R. Kessler,(2010), Multifunctional PMMA-Ceramic composites as structural dielectrics. Polymer., 51, 5823.

A. Facchetti, M.H. Yoon, T.J. Marks,(2005),Low-voltage organic transistors and inverters with ultrathin fluoropolymer gate dielectric. *Adv.Mater*., 17,1705.

ASTM D 2240: Standard Test Method for Rubber Property—Durometer Hardness.

ASTM D 3850-94: Standard Test Method for Rapid Thermal Degradation of Solid Electrical Insulating Materials by Thermo gravimetric Method (TGA).

ASTM D 792: Standard Test Methods for Density and Specific Gravity (Relative Density) of Plastics by Displacement.

ASTM D257: Standard Test Methods for DC Resistance or Conductance of Insulating Materials.

Bahaa Hussien, (2011), The D.C and A.C. Electrical properties of. PMMA-Al_2O_3 composites. *Euro.J.Sci.Res*., 52 (2),236.

C. Marius, Costache, Dongyan Wang, J.Matthew, Heidecker, E. Manias, A. Charles, Wilkie, (2006),The thermal degradation of poly(methyl methacrylate) nanocomposites with montmorillonite, layered double hydroxides and carbon nanotubes. *Polym. Adv*. Techno.,17 ,272.

Hong Wang,Feng Xiang, and Kecheng Li, (2010),Ceramic–Polymer $Ba_{0.6}Sr_{0.4}TiO_3$/Poly (Methyl Methacrylate) Composites with Different Type Composite Structures for Electronic TechnologInt. *J. Appl. Ceram. Technol.*, 7 [4] 435.

J.X. Lu, C.P. Wong,(2008), Recent Advances in High-k Nanocomposite Materials for Embedded Capacitor Applications, Dielectr.Electr. Insul., 15,1322.

K.R.S. Preethi Meher and K.B.R. Varma, (2009), Colossal dielectric behavior of semiconducting Sr_2TiMnO_6 ceramics. *Journal of applied Phys*., 105, 034113.

K.R.S. Preethi Meher, M. Savinov, S. Kamba, V. Goian and K.B.R. Varma, (2010), Structure, dielectric, and magnetic properties of Sr_2TiMnO_6 ceramics. *Journal of applied Phys*., 108,094108.

Lei Yang and Dale L.Schruben, (1994), Electrical Resistivity Behavior of Mold-Cast Metal-Filled Polymer composites. *Polym.Eng.Sci.*, 34,14.

M. A. Subramanian, D. Li, N. Duran, B.A. Reisner, A. W. Sleight,(2000),High dielectric constant in ACu3Ti4O12 and ACu3Ti3FeO12 phases *J. Solid State Chem*., 151, 323.

M. Arbatti, X. Shan, Z-Y. Cheng,(2007), Ceramic–Polymer Composites with High Dielectric Constant. *Adv. Mater*., 19, 1369.

P. Kim, S.C. Jones, P.J. Hotchkiss, J.N. Haddock, B. Kippelen, S.R. Marder, J.W. Perry,(2007),Phosphonic Acid-Modified Barium Titanate Polymer Nanocomposites with High Permittivity and Dielectric Strength. *Adv.Mater., 19, 1001.*

P. Thomas, K. T. Varughese, K. Dwarakanatha, K. B. R. Varma,(2010), Dielectric properties of Poly(vinylidene fluoride)/$CaCu_3Ti_4O_{12}$ composites. *Compos. Sci. Technol.*, 70, 539.

P. Thomas, R.S. Ernest Ravindran, K.B.R. Varma, (2012), Dielectric properties of poly(methyl methacrylate)(PMMA)/CaCu3Ti4O12 composites IEEE 10th ICPADM: 2012 Jul 24-28 2012, Bangalore, India.

Q.M. Zhang, H.F. Li, M. Poh, F. Xia, Z.Y. Cheng, H.S. Xu, C. Huang,(2002), Direct spectroscopic evidence of field-induced solid-state chain conformation transformation in a ferroelectric relaxor polymer. *Nature., 419*,284.

R. E. Newnham, D. P. Skinner, and L. E. Cross,(1978),Dielectrophoretically structured piezoelectric composites with high aspect ratio piezoelectric particles inclusions. *Mater. Res. Bull.*, 13, 525.

R. Gregorio, M. Cestari, F. E. Bernardino, (1996), Dielectric behaviour of thin films of β-PVDF/PZT and β-PVDF/$BaTiO_3$ composites. *J. Mater. Sci.*, 31, 2925.

R. Shenhar, T. B. Norsten, V. M. Rotello, (2005), Polymer-Mediated Nanoparticle Assembly: Structural Control and Applications.*Adv. Mater*., *17*, 657.

S. K. Bhattacharya and R. R. Tummala,(2000),Nanostructured barium titanate composites for embedded radio frequency applications. *J. Mater. Sci.*,11, 253.

S. Ogitani, S. A. Bidstrup, and P. A. Kohl,(2000),Improved performances of polymer-based dielectric by using inorganic/organic core-shell nanoparticles.*IEEE Trans. Adv.* Packag., 23,313.

S. U. Adikary, H. L. W. Chan, C. L. Choy, B. Sundaravel, I. H. Wilson, (2002),Characterisation of proton irradiated $Ba_{0.65}Sr_{0.35}TiO_3$/P(VDF-TrFE) ceramic–polymer composites. *Compos. Sci. Technol*., 62, 2161.

Vishal Singh, A.N. Tiwari, A.R. kulkarni, (1996), Electrical behaviour attritor processed Al/PMMA composites. *Mater. Sci .Eng*., B41,310.

Y. Bai, Z.Y. Cheng, V. Bharti, H.S. Xu, Q. Zhang, (2000),High-dielectric-constant ceramic-powder polymer composites. *Appl. Phys. Lett*., 76, 3804.

Y. Rao, S. Ogitani, P. Kohl, and C. P. Wong, (2002), Novel polymer–ceramic nanocomposite based on high dielectric constant epoxy formula for embedded capacitor application. *Appl. Polym. Sci*., 83, 1084

Z. M. Dang, Y. H. Lin, C.W Nan,(2003),Novel Ferroelectric Polymer Composites with High Dielectric Constants. *Adv. Mater*., 15, 1625.

Ziad Khattari a,n, MufeedMaghrabi a, TonyMcNally b, Saadi Abdul Jawad, (2012), A Impedance study of polymethyl methacrylate composites/multi-walled carbon nanotubes (PMMA/MWCNTs). *Physics of Condensed Matter.*, 407,759.